Scrutinizing Hall Effect in $Mn_{1-x}Fe_xSi$: Fermi Surface Evolution and Hidden Quantum Criticality

V. V. Glushkov,[1,2,*] I. I. Lobanova,[1,2] V. Yu. Ivanov,[1] V. V. Voronov,[1] V. A. Dyadkin,[3] N. M. Chubova,[4] S. V. Grigoriev,[4] and S. V. Demishev[1,2]

[1]*Prokhorov General Physics Institute of RAS, 38 Vavilov street, 119991 Moscow, Russia*
[2]*Moscow Institute of Physics and Technology, 9 Institutskiy lane, 141700 Dolgoprudny, Moscow region, Russia*
[3]*Swiss-Norwegian Beamlines at the European Synchrotron Radiation Facility, 38000 Grenoble, France*
[4]*Petersburg Nuclear Physics Institute, Gatchina, 188300 Saint-Petersburg, Russia*

(Received 18 July 2015; published 18 December 2015)

Separating between the ordinary Hall effect and anomalous Hall effect in the paramagnetic phase of $Mn_{1-x}Fe_xSi$ reveals an ordinary Hall effect sign inversion associated with the hidden quantum critical (QC) point $x^* \sim 0.11$. The effective hole doping at intermediate Fe content leads to verifiable predictions in the field of fermiology, magnetic interactions, and QC phenomena in $Mn_{1-x}Fe_xSi$. The change of electron and hole concentrations is considered as a "driving force" for tuning the QC regime in $Mn_{1-x}Fe_xSi$ via modifying the Ruderman-Kittel-Kasuya-Yosida exchange interaction within the Heisenberg model of magnetism.

DOI: 10.1103/PhysRevLett.115.256601 PACS numbers: 72.15.Gd, 75.30.Kz

Studying the ordinary Hall effect (OHE) in the quantum critical (QC) regime is an important tool, which allows choosing between various scenarios of non-Fermi liquid behavior in various strongly correlated electron systems [1–5]. In the case of localized magnetic moments (LMM) a collapse of the Fermi surface (FS) expected exactly at the quantum critical point (QCP) results in an abrupt change of the Hall constant at zero temperature [3,4]. In contrast, no direct evidence of the Lifshitz transition at QCP [5] is provided for itinerant magnets in the spin density wave model of quantum criticality [4].

This apparent distinction between localized and itinerant behavior stimulates a particular interest to the study of OHE in $Mn_{1-x}Fe_xSi$ solid solutions. Recently, comprehensive neutron scattering study [6,7] together with magnetic data [8–10] and specific heat measurements [9] discovered a QCP corresponding to the suppression of the spiral phase with long-range magnetic order (LRO) in $Mn_{1-x}Fe_xSi$. This QCP located at $x^* \sim 0.11$–0.12 [Fig. 1(a)] [6–10] is hidden by a surrounding phase with a short-range magnetic order (SRO) [7,9,10] that agrees well with the theoretical models [11,12]. This SRO phase, referred to sometimes as chiral spin liquid [11], is destroyed at the second QCP $x_c \sim 0.24$ (Fig. 1) [10]. The diverging of magnetic susceptibility $\chi(T) \sim 1/T^{\xi}(\xi = 0.5$–$0.6)$ at $x > x_c$ [11] is proved to be a fingerprint of the disorder-driven Griffiths (G) phase consisting of separated spin clusters [13,14]. So not only the modulation of exchange interactions, which seems to induce the first QCP at x^* [7,10], but also strong disorder effects impact significantly on quantum criticality in $Mn_{1-x}Fe_xSi$.

However, some essential features of QC behavior in this system have not been recognized up to now. First, the critical temperature of the LRO phase $T_c(x)$ does not follow the x dependence of the ferromagnetic (F) exchange $J(x)$, which turns zero for Fe content exceeding x^* [Fig. 1(a)] [6]. As long as LRO in $Mn_{1-x}Fe_xSi$ originates from the competing F exchange and Dzyaloshinskii-Moriya interaction (DMI) [6,7] and DMI does not result in any magnetic ordering itself, the different behavior of $T_c(x)$ and $J(x)$ indicates an intrinsic complexity of magnetic interactions in $Mn_{1-x}Fe_xSi$. Second, the magnetic subsystem of $Mn_{1-x}Fe_xSi$ is fragmented into spin clusters at $x_c \sim 0.24$ [10]. Although this experimental fact may be explained as a percolation-type transition [10], the most probable neighbor of Mn magnetic ion in the treated concentration range is a Mn magnetic ion as well. So the factors driving the change in the topology, which results in the formation of the Griffiths phase, need to be clarified. Third, despite the fact that the $Mn_{1-x}Fe_xSi$ solid solutions are often considered as itinerant magnets [11,12], local-density approximation calculations [15] and recent magnetic resonance and magnetoresistance studies [16,17] favor the alternative explanation based on the Heisenberg LMM of Mn ions. Therefore, the different behavior of the Hall effect in QC systems with LMM and itinerant magnets [3–5] makes it possible to shed more light on the microscopic mechanisms of quantum criticality in $Mn_{1-x}Fe_xSi$.

This Letter addresses the aforementioned problems through the study of the Hall effect in the paramagnetic (P) phase of $Mn_{1-x}Fe_xSi$ [Fig. 1(a)]. Currently, a noticeable discrepancy (about two times) in the electron concentration is reported, even for pure MnSi [18,19]. Moreover, the recent study of the Hall effect in $Mn_{1-x}Fe_xSi$ has initiated a pessimistic conclusion that any correct Hall constant can

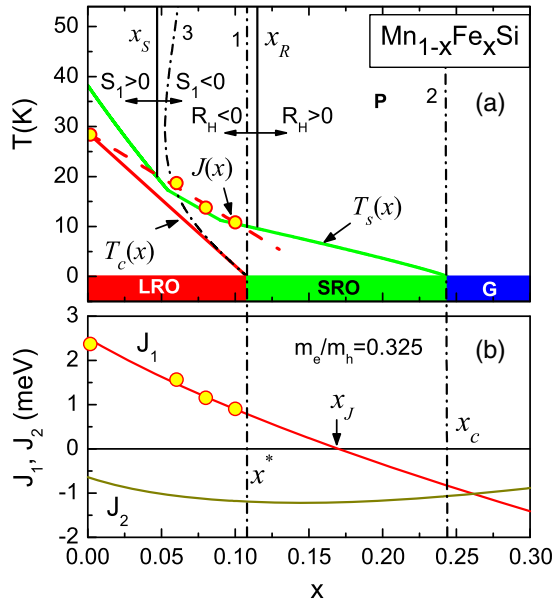

FIG. 1 (color online). (a) $Mn_{1-x}Fe_xSi$ magnetic phase diagram. The paramagnetic (P) phase corresponds to $T > T_s(x)$, $T_s(x)$ is the onset of SRO. The LRO phase boundary $T_c(x)$ [7,10] is supplemented with the $T_c(0)J(x)/J(0)$ data plotted from the experimental values of exchange energy [6]. Solid lines at x_S and x_R (P phase) separate the different regimes of AHE and OHE (see text for details). Dash-dotted lines mark (1) the hidden QCP $x^* \sim 0.11$, (2) the SRO suppression at $x_c \sim 0.24$, and (3) the crossover between classic and quantum fluctuations [10]. (b) The estimated nn $J_1(r_1)$ and nnn $J_2(r_2)$ exchange constants in $Mn_{1-x}Fe_xSi$ ($m_e/m_h = 0.325$). Circles represent the experimental $J(x)$ data [7]

hardly be estimated because OHE in this system is much less than the anomalous Hall effect (AHE) [20]. This difficulty is shown to be overcome by the implementation of the data analysis developed recently for MnSi [21] allowing the reliable determination of the OHE and AHE contributions from experiment.

Experimental details and the set of Hall resistivity $\rho_H(B,T)$ and magnetization $M(B,T)$ data are resummarized in the Supplemental Material [22]. Low field Hall resistivity extracted from the $\rho_H(B,T_0)$ data for $B_0 = 0.5T$ [Fig. 2(a)] shows clearly that ρ_H decreases with the lowering of temperature in the P phase for all studied crystals. Distinct anomalies in the $\rho_H(T)$ data are identified at the transition into the SRO phase [arrows in Fig. 2(a)]. The most prominent downturn of low temperature Hall resistivity occurs for $x = 0.194$ close to the SRO phase boundary at the second QCP $x_c \sim 0.24$ [Fig. 2(a)].

The strong $\rho_H(T)$ dependences [Fig. 2(a)] allow applying the procedure developed earlier to separate between OHE and AHE in the P phase of MnSi [21]. The functional form of the anomalous term $\rho_H^a = \mu_0 S_n \rho^n M$ in $\rho_H = R_H B + \rho_H^a$ depends on the scattering mechanism of charge carriers [26]. For $Mn_{1-x}Fe_xSi$ the exponent $n = 2$ corresponds to the intrinsic AHE related to the k-space Berry phase, whereas extrinsic side-jump scattering (which gives the same value of n) is small [20,26,27]. The case of $n = 1$ is associated with skew scattering on LMM due to spin-orbit coupling [26].

A comparison of the $\rho_H(T,B_0)$ data within these AHE scenarios suggests that the best approximation corresponds to $\rho_H/B_0 = f(\rho M/B_0)$ plots [Fig. 2(b)]. So Hall resistivity in the P phase of $Mn_{1-x}Fe_xSi$ acquires the form $\rho_H = R_H B + \mu_0 S_1 \rho M$ with the fixed values of R_H and S_1 extracted from the linear fit in the proper graph for each composition [Fig. 2(b)]. The obtained $R_H(x)$ and $S_1(x)$ dependences are presented in [Fig. 2(c)]. The validity of the above analysis is supported by excellent agreement between experimental $\rho_H(T,B_0)$ curves and these that are calculated from resistivity and magnetization by using the found OHE and AHE coefficients [Fig. 2(a)]. It is spectacular that the rising of Fe content results in the opposite trends of OHE and AHE changing their signs in the P phase [see the insets in Figs. 2(b) and 2(c)]. Note that the S_1 sign inversion occurs at the concentration of $x_S \sim 0.05$ much lower than that of R_H [$x_R \approx 0.115$, Fig. 2(c)]. The boundary dividing the $S_1 > 0$ and $S_1 < 0$ regions is very close to the crossover between classical and QC fluctuations [line 3 in Fig. 1(a)] predicted for $Mn_{1-x}Fe_xSi$ [10]. This crossover induced by the hidden QCP is also detected from resistivity data, which are sensitive to the scattering regime of charge carriers [10]. Therefore, it is possible to suppose that the change of magnetic scattering on spin fluctuations taking place at the crossover line affects the skew-scattering contribution to AHE and may be responsible for its observed inversion in $Mn_{1-x}Fe_xSi$. However, no relevant theory describing this effect is available at this moment.

The other important finding appears from the OHE sign inversion detected at Fe content $x_R \approx 0.115$ [Fig. 2(c)]. This fact points to the competing electron and hole contributions to charge transport in $Mn_{1-x}Fe_xSi$. Note that the boundary between negative ($R_H < 0, x < x_R$) and positive ($R_H > 0$, $x > x_R$) OHE coincides with the hidden QCP $x = x^* \approx 0.11$ [Fig. 1(a), line 1]. Such an inversion of OHE may result from the change of the FS topology in strong magnetic fields, when the inversed cyclotron frequency is much less than the electrons τ_e and holes τ_h relaxation times. In this case, the corresponding Lifshitz transition at QCP would favor a scenario based on the Heisenberg-type model of magnetism [3].

However, this possibility does not likely meet the case of $Mn_{1-x}Fe_xSi$. First, the data in Fig. 2 correspond evidently to weak magnetic fields. Considering the effective concentrations $n(x)$ and $p(x)$ and mobilities $\mu_e(x)$ and $\mu_h(x)$ for electrons and holes, respectively, the condition for OHE sign inversion in the degenerate limit $p(x_R) - b(x_R)^2 n(x_R) = 0$ [28] depends on the mobilities ratio $b(x) = |\mu_e(x)/\mu_h(x)|$. Second, high electron effective mass $m_e \sim 17 m_0$ [29] makes it difficult to reach the high

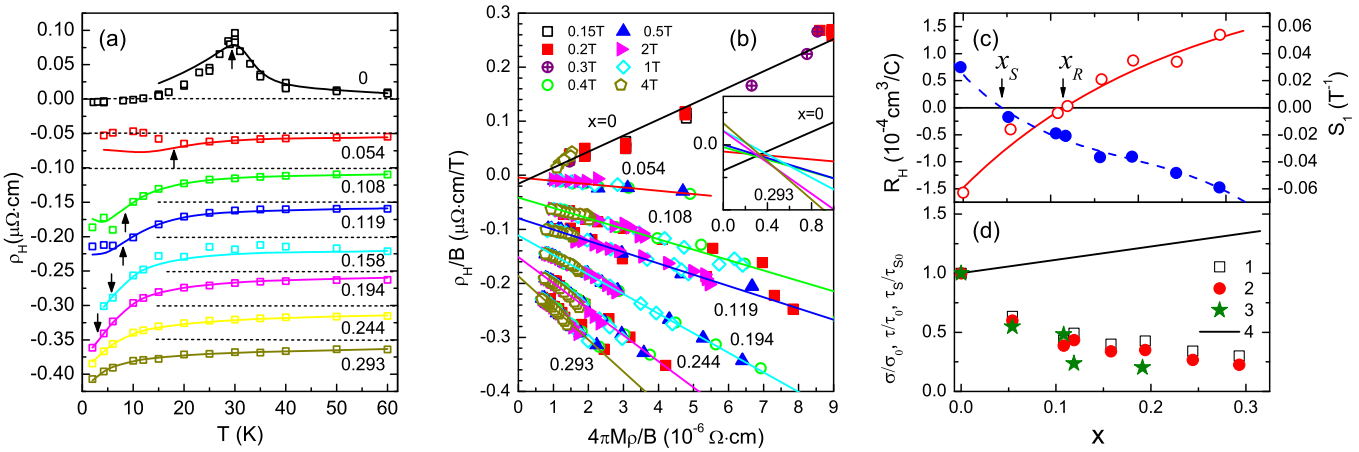

FIG. 2 (color online). (a) Hall resistivity $\rho_H(T, B_0)$ for pure MnSi ($B_0 = 0.31$ T) and $Mn_{1-x}Fe_xSi$ ($B_0 = 0.5$ T). Arrows indicate the onset of SRO at $T_s(x)$. Solid lines are the fits by $\rho_H = R_H B_0 + \mu_0 S_1 \rho M$ with $R_H(x)$ and $S_1(x)$ shown in panel (c). For clarity, the $\rho_H(x > 0)$ data are shifted down by 50 nΩ cm. (b) Scaling plots of Hall resistivity $\rho_H/B_0 = f(\mu_0 S_1 \rho M/B_0)$ in the P phase of $Mn_{1-x}Fe_xSi$ solid solutions. Solid lines are the best linear fits of the data. For clarity, the data for $x > 0.1$ are shifted down by 40 nΩ cm/T for each composition. The inset enlarges the intersections of the unmoved best fits with y axis. (c) Hall constant R_H (open circles) and AHE coefficient S_1 (filled circles) in $Mn_{1-x}Fe_xSi$. The solid line is the fit by Eq. (1). (d) Reduced conductivity $\sigma(x)/\sigma(0)$ (1), electron transport relaxation time $\tau(x)/\tau(0)$ (2), and spin relaxation time $\tau_S(x)/\tau_S(0)$ [17,25] (3) for $T = 30$ K. Line 4 is the $\sigma(x)/\sigma(0)$ dependence expected for $\tau_e(x) = \text{const}$.

magnetic field regime. Therefore, the observed $R_H(x)$ sign inversion does not exclude the itinerant origin of Hall effect peculiarities [5]. At the same time the OHE evolution in $Mn_{1-x}Fe_xSi$ suggests that the substitution of Mn with Fe results in the effective hole doping so that the FS definitely evolves. This opportunity is not foreseen in any models of QC phenomena in MnSi based solids [11,12].

Quantitative information about the FS evolution crucial for the analysis of the QC phenomena in $Mn_{1-x}Fe_xSi$ can be extracted from our $R_H(x)$ data under some model assumptions. First, the main effect of substitution of Mn by Fe is suggested to be the change of electron n and hole p concentrations. This hypothesis based on the experimental data [Fig. 2(c)] means that electrons are associated with manganese, whereas holes are supplied by iron. The simplest case assumes $n(x) = n(0)(1 - x)$ and $p(x) = p_1 x$ (p_1 is some coefficient). Second, the $b(x) = |\mu_e(x)/\mu_h(x)|$ ratio is treated as a constant for the studied concentrations. The latter supposition to be an apparently rather rough approximation is argued below.

For $b(x) = \text{const}$ the expression for two groups of charge carriers [28] may be reduced to

$$R_H(x) = R_H(0)\frac{1 - x/x_R}{(1 + ax/x_R)^2}, \qquad (1)$$

with $R_H(0) = -[n(0)|e|]^{-1}$ and $a = b(1 - x_R) - x_R$. $R_H(x_R) = 0$ fixes the value of $p_1 = n(0)b_2(1 - x_R)/x_R$. For $x_R \approx 0.115$ two parameter fitting by Eq. (1) describes reasonably the $R_H(x)$ data with $R_H(0) = (1.48 \pm 0.16) \times 10^{-4}$ cm^3/C and $a = 0.13 \pm 0.04$ ($b \approx 0.28$) [solid line in Fig. 2(c)]. The nice correlation of the fit with the $R_H(x)$ points [Fig. 2(c)] proves our supposition for $b(x) = \text{const}$.

Another feature can be captured from the concentration dependence of conductivity $\sigma(x)$ in $Mn_{1-x}Fe_xSi$. Allowing for $b = m_h\tau_e/m_e\tau_h = \text{const}$ ($m_{e,h}$ and $\tau_{e,h}$ are effective masses and relaxation times for electrons and holes) the total conductivity may be expressed as

$$\sigma(x) = \sigma(0)(1 + \gamma x)\tau_e(x)/\tau_e(0), \qquad (2)$$

where $\gamma = b(1/x_R - 1) - 1 \approx 1.13$. For $\tau_e(x) = \text{const}$ conductivity is expected to increase linearly with x [line 4 in Fig. 2(d)]. So a pronounced decrease of the $\sigma(x)/\sigma(0)$ ratio found at $x < 0.3$ for $T = 30$ K [squares in Fig. 2(d)] suggests the strong concentration dependence of relaxation time as estimated from Eq. (2) [circles in Fig. 2(d)]. As scattering on spin fluctuations dominates in $Mn_{1-x}Fe_xSi$ [10,16,17], it is reasonable to suppose that this mechanism equally affects electrons and holes providing a constant ratio of their mobilities and relaxation times. Because spin fluctuations control also the electron spin resonance linewidth $W(x)$ in $Mn_{1-x}Fe_xSi$ [17], $\tau_{e,h} \sim 1/W(x)$ is expected in the considered model. The data set of $\tau_S(x)/\tau_S(0) \sim W(0)/W(x)$ [17,25] [stars in Fig. 2(d)] demonstrates evident correlation between the $\tau_S(x)$ and $\tau(x)$ behavior [Fig. 2(d)] that can be considered as an additional justification for the suggested model.

In our results, iron doping fills the hole FS pocket and therefore, as long as holes are missing in pure MnSi, Lifshits transition occurs formally at $x = 0$ not relating to the hidden QCP x^*. This result appears to be nontrivial because the substitution of Mn by Fe should add electrons

to $Mn_{1-x}Fe_xSi$ and hence electron doping rather than hole one may be expected. However, in the analyzed temperature diapason the case $x = 1$ (pure FeSi) corresponds to p-type conductivity proven by the Hall effect [30–32] and thermopower [32,33] data. Therefore, the doping effect discovered in the present work meets available experiments. From the theoretical point of view the spectrum around Fermi energy in $Mn_{1-x}Fe_xSi$ is formed by ten very flat bands resulting from the combination of $3d$ (Mn, Fe) and $3s$, $3p$ (Si) states [34,35]. Because of the complexity of the problem, *ab initio* calculations available up to now have provided no reliable estimates of charge carriers' concentrations and signs either for MnSi or for FeSi [34–37]. The additional difficulty appears to be due to the necessity of the correct accounting of the Coulomb repulsion and the valence fluctuation suppression effect [38]. Nevertheless, we believe that advanced band structure calculations for $Mn_{1-x}Fe_xSi$ will be rewarding and the results of the present work may serve as a "reference point" in further theoretical analysis.

The essential factor for stimulating of any *ab initio* calculations is the availability of the quantitative criteria for the $Mn_{1-x}Fe_xSi$ band structure. This option cannot be obviously provided by the estimated mobility ratio $b = 0.28$ due to the lack of the $\tau_{e,h}$ values. The final part of the Letter shows that such a criteria may be obtained from the careful analysis of exchange interactions in $Mn_{1-x}Fe_xSi$.

Although these compounds are generally treated as itinerant magnets, few works discuss the microscopic "driving force" for QC phenomena for MnSi-based solids in the itinerant paradigm not allowing for any possibility of FS transformation [12]. On the contrary, the discovered change of electron and hole concentrations under the substitution of Mn by Fe should result in the modulation of effective Ruderman-Kittel-Kasuya-Yosida (RKKY) exchange within the Heisenberg picture of magnetism. Note that magnetic interactions in $3d$ metals are not generally described by the RKKY approach due to the itinerant origin of magnetism [39]. However, we cannot ignore clear evidence for LMMs of Mn in $Mn_{1-x}Fe_xSi$ deduced from experiment or postulated in theory [15–17,25].

The extending of the general expression for the RKKY interaction [39] to the two groups of charge carriers with quadratic isotropic dispersion results in

$$J(x,r) = J(0,r)\frac{\varphi[\alpha(r)(1-x)^{1/3}] + (m_h/m_e)\varphi[\alpha'(r)x^{1/3}]}{\varphi[\alpha(r)]}, \tag{3}$$

with $\varphi(z) = z\cos(z) - \sin(z)$, $\alpha(r) = 2k_{Fe}(0)r$, and $\alpha'(r) = \alpha(r)(a + x_R)^2/[x_R(1 - x_R)]$ (see [22] for details). In this model the nearest neighbor (nn) exchange for $x = 0$ in the B20 structure happens to be ferromagnetic $J_1(r_1 = 2.80\ \text{Å}) > 0$, whereas the next nearest neighbor (nnn) exchange is antiferromagnetic (AF) and $J_2(r_2 = 4.39\ \text{Å}) < 0$ [Fig. 1(b); see [22,40] for details].

Fitting of the experimental $J(x)$ data for $Mn_{1-x}Fe_xSi$ [7] by Eq. (3) shows that the hole contribution (the second term in the nominator) is important as long as it stays negative and its absolute value increases noticeably with x. At the same time the tiny variation of electron term in the nominator does not account for the experimental $J(x)$ evolution [circles in Fig. 1(b)]. The best fit of the $J_1(x)$ data within Eq. (3) [line 1 in Fig. 1(b)] corresponds to $m_e/m_h = 0.325$, which may serve as a reference value for band structure calculations. If m_e/m_h is fixed Eq. (3) gives the nnn exchange $J_2(x) = J(x, r_2)$ [line 2 in Fig. 1(b)] without any additional parameters.

The $J_1(x)$ and $J_2(x)$ evolution with Fe doping allows us to state some other important findings. First, the nn exchange changes sign at $x_J \sim 0.17$ [Fig. 1(b)]. Thus, the FS transformation in $Mn_{1-x}Fe_xSi$ is proved to tune effectively the magnetic interaction from $F\ J_1(x < x_J) > 0$ to AF $J_1(x > x_J) < 0$. Second, the opposite signs of J_1 and J_2 for $x < x_J$ and the same signs of J_1 and J_2 for $x > x_J$ mean the strong influence of frustration on the magnetic properties of $Mn_{1-x}Fe_xSi$ pointed out earlier for MnSi based solids [41]. Because the absolute values of J_1 and J_2 are equal near QCPs x^* and x_c, frustration should essentially affect the resultant spin configuration. So the discrepancy between $T_c(x)$ and $J(x)$ [4] [Fig. 1(a)] may be induced by the nnn AF interaction. The strong frustration effects are also expected in the "tail" of the SRO phase (Fig. 1) facilitating segmentation into spin clusters and the formation of a Griffiths phase for $x > x_c$ [10].

In summary, the novel approach to the Hall effect study in the P phase of $Mn_{1-x}Fe_xSi$ allowed finding the dependences of the OHE and AHE constants R_H and S_1 on the Fe content. Hole doping induced by the substitution of Mn with Fe proves that two groups of charge carriers contribute to OHE in $Mn_{1-x}Fe_xSi$. The fact that the observed $R(x)$ and $S_1(x)$ sign inversions are definitely associated with the hidden QCP $x^* \sim 0.11$ reveals the relationship of these transport anomalies to the QC transition between LRO and SRO phases.

Our quantitative analysis leads to some predictions in the field of fermiology, magnetic interactions, and QC phenomena in $Mn_{1-x}Fe_xSi$ to be verified by experiments. In particular, the rising of Fe content is expected to reduce the electron FS section filling the pocket with heavier holes ($m_h/m_e \approx 3$). The discovered FS evolution is not foreseen by the itinerant models of quantum criticality in $Mn_{1-x}Fe_xSi$ [11,12]. On the contrary, the LMM approach predicts a strong frustration affecting the position of the hidden QCP $x^* \sim 0.11$ and facilitating (together with the disorder) the SRO suppression and the formation of the G phase for $x > x_c \sim 0.24$. As long as the exchange energies are tuned via the RKKY mechanism, the change of electron and hole concentrations may be considered as a

microscopic driving force for QC in $Mn_{1-x}Fe_xSi$. In this respect, the smooth redistribution between the electron and hole FS pockets established for $x < 0.3$ in this work needs to be independently verified by rigorous band calculations and angle-resolved photoemission spectroscopy experiments.

The most striking consequence of the LMM approach is the F to AF $J_1(x)$ evolution occurring in $Mn_{1-x}Fe_xSi$ at $x_J \sim 0.17$. The different types of magnetic interactions modulated by Fe content make the SRO phase inhomogeneous in the range $x^* < x < x_c$. Simultaneously, the G phase $(x > x_c)$ should be constructed from AF rather than F spin clusters. Besides, the DMI and the spiral structures need to be treated by different ways for $x > x_J$ and $x < x_J$. As far as this unusual behavior can be hardly expected in itinerant models [11,12], verifying of this prediction may be considered as an *experimentum crucius* for Heisenberg-type models of magnetism suggested for $Mn_{1-x}Fe_xSi$.

The authors are grateful to D. I. Khomskii and N. E. Sluchanko for stimulating discussions. This work was supported by the RAS Programmes "Electron spin resonance, spin-dependent electronic effects and spin technologies," "Electron correlations in strongly interacting systems," and by RFBR Grant No. 13-02-00160.

*glushkov@lt.gpi.ru

[1] A. Yeh, Y.-A. Soh, J. Brooke, G. Aeppli, T. F. Rosenbaum, and S. M. Hayden, Nature (London) **419**, 459 (2002).
[2] M. Lee, A. Husmann, T. F. Rosenbaum, and G. Aeppli, Phys. Rev. Lett. **92**, 187201 (2004).
[3] S. Paschen, T. Lühmann, S. Wirth, P. Gegenwart, O. Trovarelli, C. Geibel, F. Steglich, P. Coleman, and Q. Si, Nature (London) **432**, 881 (2004).
[4] S. Friedemann, N. Oeschler, S. Wirth, C. Krellner, C. Geibel, F. Steglich, S. Paschen, S. Kirchner, and Q. Si, Proc. Natl. Acad. Sci. U.S.A. **107**, 14547 (2010).
[5] T. Combier, D. Aoki, G. Knebel, and J. Flouquet, J. Phys. Soc. Jpn. **82**, 104705 (2013).
[6] S. V. Grigoriev, V. A. Dyadkin, E. V. Moskvin, D. Lamago, Th. Wolf, H. Eckerlebe, and S. V. Maleyev, Phys. Rev. B **79**, 144417 (2009).
[7] S. V. Grigoriev, E. V. Moskvin, V. A. Dyadkin, D. Lamago, Th. Wolf, H. Eckerlebe, and S. V. Maleyev, Phys. Rev. B **83**, 224411 (2011).
[8] Y. Nishihara, S. Waki, and S. Ogawa, Phys. Rev. B **30**, 32 (1984).
[9] A. Bauer, A. Neubauer, C. Franz, W. Münzer, M. Garst, and C. Pfleiderer, Phys. Rev. B **82**, 064404 (2010).
[10] S. V. Demishev, I. I. Lobanova, V. V. Glushkov, T. V. Ischenko, N. E. Sluchanko, V. A. Dyadkin, N. M. Potapova, and S. V. Grigoriev, JETP Lett. **98**, 829 (2014).
[11] S. Tewari, D. Belitz, and T. R. Kirkpatrick, Phys. Rev. Lett. **96**, 047207 (2006).
[12] F. Kruger, U. Karahasanovic, and A. G. Green, Phys. Rev. Lett. **108**, 067003 (2012).
[13] A. Bray, Phys. Rev. Lett. **59**, 586 (1987).
[14] R. Griffiths, Phys. Rev. Lett. **23**, 17 (1969).
[15] M. Corti, F. Carbone, M. Filibian, Th. Jarlborg, A. A. Nugroho, and P. Carretta, Phys. Rev. B **75**, 115111 (2007).
[16] S. V. Demishev, V. V. Glushkov, I. I. Lobanova, M. A. Anisimov, V. Yu Ivanov, T. V. Ishchenko, M. S. Karasev, N. A. Samarin, N. E. Sluchanko, V. M. Zimin, and A. V. Semeno, Phys. Rev. B **85**, 045131 (2012).
[17] S. V. Demishev, A. N. Samarin, V. V. Glushkov, M. I. Gilmanov, I. I. Lobanova, N. A. Samarin, A. V. Semeno, N. E. Sluchanko, N. M. Chubova, V. A. Dyadkin, and S. V. Grigoriev, JETP Lett. **100**, 28 (2014).
[18] M. Lee, Y. Onose, Y. Tokura, and N. P. Ong, Phys. Rev. B **75**, 172403 (2007).
[19] A. Neubauer, C. Pfleiderer, B. Binz, A. Rosch, R. Ritz, P. G. Niklowitz, and P. Böni, Phys. Rev. Lett. **102**, 186602 (2009).
[20] C. Franz, F. Freimuth, A. Bauer, R. Ritz, C. Schnarr, C. Duvinage, T. Adams, S. Blügel, A. Rosch, Y. Mokrousov, and C. Pfleiderer, Phys. Rev. Lett. **112**, 186601 (2014).
[21] V. V. Glushkov, I. I. Lobanova, V. Yu. Ivanov, and S. V. Demishev, JETP Lett. **101**, 459 (2015).
[22] See Supplemental Material at http://link.aps.org/supplemental/10.1103/PhysRevLett.115.256601, which includes Refs. [23,24], for experimental details and data as well for estimating exchange constants.
[23] V. V. Rylkov, S. N. Nikolaev, K. Yu. Chernoglazov, B. A. Aronzon, K. I. Maslakov, V. V. Tugushev, E. T. Kulatov, I. A. Likhachev, E. M. Pashaev, A. S. Semisalov, N. S. Perov, A. B. Granovskii, E. A. Ganshina, O. A. Novodvorskii, O. D. Khramova, E. V. Khaidukov, and V. Ya. Panchenko, JETP Lett. **96**, 255 (2012).
[24] A. Aharoni, J. Appl. Phys. **83**, 3432 (1998).
[25] S. V. Demishev, A. V. Semeno, A. V. Bogach, V. V. Glushkov, N. E. Sluchanko, N. A. Samarin, and A. L. Chernobrovkin, JETP Lett. **93**, 213 (2011).
[26] N. Nagaosa, J. Sinova, S. Onoda, A. H. MacDonald, and N. P. Ong, Rev. Mod. Phys. **82**, 1539 (2010).
[27] Y. Li, N. Kanazawa, X. Z. Yu, A. Tsukazaki, M. Kawasaki, M. Ichikawa, X. F. Jin, F. Kagawa, and Y. Tokura, Phys. Rev. Lett. **110**, 117202 (2013).
[28] K. Seeger, *Semiconductor Physics* (Springer-Verlag, Vienna, 1973).
[29] F. P. Mena, D. van der Marel, A. Damascelli, M. Fath, A. A. Menovsky, and J. A. Mydosh, Phys. Rev. B **67**, 241101(R) (2003).
[30] S. Paschen, E. Felder, M. A. Chernikov, L. Degiorgi, H. Schwer, H. R. Ott, D. P. Young, J. L. Sarrao, and Z. Fisk, Phys. Rev. B **56**, 12916 (1997).
[31] N. E. Sluchanko, V. V. Glushkov, S. V. Demishev, M. V. Kondrin, K. M. Petukhov, A. A. Pronin, N. A. Samarin, Y. Bruynseraede, V. V. Moshchalkov, and A. A. Menovsky, JETP Lett. **68**, 817 (1998).
[32] J. F. DiTusa, K. Friemelt, E. Bucher, G. Aeppli, and A. P. Ramirez, Phys. Rev. B **58**, 10288 (1998).
[33] N. E. Sluchanko, V. V. Glushkov, S. V. Demishev, M. V. Kondrin, K. M. Petukhov, N. A. Samarin, V. V. Moshchalkov, and A. A. Menovsky, Europhys. Lett. **51**, 557 (2000).
[34] L. Taillefer, G. Lonzarich, and P. Strange, J. Magn. Magn. Mater. **54–57**, 957 (1986).

[35] D. van der Marel, A. Damascelli, K. Schulte, and A. A. Menovsky, Phys. B Condens. Matter **244**, 138 (1998).
[36] V. I. Anisimov, R. Hlubina, M. A. Korotin, V. V. Mazurenko, T. M. Rice, A. O. Shorikov, and M. Sigrist, Phys. Rev. Lett. **89**, 257203 (2002).
[37] V. V. Mazurenko, A. O. Shorikov, A. V. Lukoyanov, K. Kharlov, E. Gorelov, A. I. Lichtenstein, and V. I. Anisimov, Phys. Rev. B **81**, 125131 (2010).
[38] F. Carbone, M. Zangrando, A. Brinkman, A. Nicolaou, F. Bondino, E. Magnano, A. A. Nugroho, F. Parmigiani, Th. Jarlborg, and D. van der Marel, Phys. Rev. B **73**, 085114 (2006).
[39] S. Vonsovskii, *Magnetism* (J. Wiley & Sons, New York, 1974), Vol. 2.
[40] S. V. Grigoriev, D. Chernyshov, V. A. Dyadkin, V. Dmitriev, E. V. Moskvin, D. Lamago, Th. Wolf, D. Menzel, J. Schoenes, S. V. Maleyev, and H. Eckerlebe, Phys. Rev. B **81**, 012408 (2010).
[41] J. M. Hopkinson and H. Y. Kee, Phys. Rev. B **75**, 064430 (2007).